Comparison of the Importance Sampling Single Chain Mean Field Theory with Monte Carlo Simulation and Self-Consistent Field Calculations for Polymer Adsorption onto a Flat Wall

Josep Bonet Avalos,* Allan D. Mackie, and Silvia Díez-Orrite

Departament d'Enginyeria Química, ETSEQ, Universitat Rovira i Virgili, Avinguda dels Països Catalans, 26; 43007 Tarragona, Spain

Received March 19, 2003; Revised Manuscript Received November 3, 2003

ABSTRACT: The single chain mean field theory (SCMF) with importance sampling methodology has been applied to study homopolymer adsorption onto flat interfaces. A comparison with recent Monte Carlo data reveals that the excluded volume correlations along the chain are crucial in quantitatively reproducing the observed structure of the layer. The SCMF approach introduces a sampling of the self-avoiding one-chain conformations in a self-consistent mean-field, that allows for the local swelling of the chain. Unlike classical self-consistent field approaches, based on ideal chain statistics, the correct spatial as well as bulk density dependence of the profiles and structure are recovered by the SCMF approach.

1. Introduction

The internal equilibrium structure of reversibly adsorbed polymers is still a matter of debate that is in need of much clarifying experimental and theoretical work to reveal all of its internal complexity. Pioneering works on this topic include those of Jones and Richmond[1] which, starting from the mean-field treatment of Edwards,[2,3] introduced the *ground-state dominance* approximation.[4,5] In this formalism, a free energy functional for a one-order parameter is constructed from which the monomer density profile is derived. Later, de Gennes,[6] using a free energy functional based on the Cahn−Hilliard theory, was able to reproduce the proper scaling laws in the profile. Both free energy functionals, however, are essentially mean-field and depend on one single-order parameter and no finite size effects are described since the chains are formally infinite.

Subsequent numerical[7] and theoretical[8−10] work, based on the self-consistent field approach of Edwards, but without some of the simplifications of the free energy functionals described, indicated that the structure of the layer is more complex than suggested by the one-order parameter approaches mentioned. This complexity is due to the important finite size effects that give a particular importance to the polymer end points, completely disregarded in the one order parameter theories, which essentially describe the formation of polymeric loops on the surface. Results from the self-consistent field numerical method of Scheutjens and Fleer on polymer adsorption onto flat surfaces, as well as the theoretical treatment based on two-order parameters of Semenov, Joanny, Johner, and collaborators, show a division of the layer into a inner loop-dominant and an outer tail-dominant subregions. A consequence of this segregation is the existence of a characteristic length of the layer, namely z^*, that governs the scaling of the *central* region of the adsorbed profile. However, although the qualitative information given by the mean-field theories based on Edwards equation is of great interest, they fail in reproducing the scaling exponents[8] and experimental data.[11] The ideal character of the chains in the mean field is a description which is only valid in $d \geq 4$, and the exponents found by these theories are thus consistent with this fact. The excluded volume correlations along the reference chain backbone are treated only on average and the chain keeps the Markovian character of an ideal (overlapping) chain.

In this paper, we will use the SCMF approach developed in ref 12 to analyze the equilibrium behavior of polymer adsorption onto flat interfaces. We will pay special attention to the comparison with recent Monte Carlo data[13] that has revealed many interesting aspects of the adsorbed layer behavior, especially for relatively short chains, far from the scaling limit $N \rightarrow \infty$, where no simple analytical theory exists to predict the dependence of the profiles with the bulk density.

As far as the effect of the excluded volume correlations is concerned, one can say that the ideal (Markovian) nature of the Edwards approach is responsible for the fact that the exponents obtained in the different power law regimes disagree with scaling results[8] and experimental data.[11] Thus, in addition to the aforementioned self-consistent field calculations, more detailed theoretical analysis, based on the renormalization group,[14,15] and computational work, such as Monte Carlo simulations (MC), have been required,[16−20] aiming at a more quantitative comparison with the experimentally observable power-law decay of the profiles. In addition, scaling laws are concerned with very long polymers, $N \rightarrow \infty$, often lying out of the range of experimentally accessible polymer sizes. Thus, it is also of crucial interest to analyze the behavior of shorter polymers.

Monte Carlo simulations of polymer adsorption are very difficult due to the large energetic barriers to be overcome by polymers in the sampling of its configurational space. The relaxation of the structural details of the adsorbed layer is a difficult matter that has been responsible for the fact that only a few MC analysis have been done for the adsorption of relatively long polymers (hundreds of segments). In fact, MC results are found only from the beginning of the past decade. One has, for instance, short polymers of $N = 32$[17] adsorbed onto a flat wall, or results for longer chains,[16] which have some disagreements with respect to most of the modern MC data.[20] In this context, the SCMF theory appears to be a suitable tool to analyze long polymer adsorption.

10.1021/ma034349t CCC: $27.50
Published on Web 01/03/2004

The advantages of this method are, on one hand, that it includes excluded volume correlations along the chain and thus proper scaling laws are expected to be found in the long chain limit. On the other hand, the sampling of the configurational space of one single chain in a mean field is much simpler than many body MC simulations and, thus, can be more efficiently carried out.

In this paper, we will apply the SCMF theory, with the importance sampling developed in ref 12, to polymer adsorption onto a plane wall. The results obtained will be compared with Monte Carlo simulations under the same conditions in order to analyze the differences between the two methods and prove the predictive nature of the method. Moreover, SCMF results with the generation of overlapping (ideal) chains will be compared with Markovian self-consistent field data obtained from the application of the Scheutjens−Fleer theory. This comparison will serve us to study the importance of the excluded volume correlations along the chain and thus the role of the Markovian/non-Markovian nature of the conformation of the chain used as the reference state, as far as the layer properties are concerned.

The rest of the paper is organized as follows. In section 2, we will summarize the theory underlying the SCMF theory with the importance sampling development discussed in ref 12. In section 3, the structure of the adsorbed layer will be analyzed from our SCMF methodology and compared with MC simulations data as well as with data from the Scheutjens and Fleer method, for different bulk volume fractions. Finally, in section 4, we will discuss the main points arising from this work.

2. The Single Chain Mean Field Theory

The most important characteristic of the SCMF theory is the generation of independent self-avoiding chain conformations of known statistical weight, depending upon the physical conditions, from which the relevant averages are calculated.[21−26] By retaining the explicit self-avoidance of the chain conformation, the non-Markovian nature of the chain propagator can be accounted for even at a mean field level. Classical self-consistent field theories (SCF) are based on the calculation of a Markovian chain propagator, which follows ideal chain properties, disregarding correlations along the chain backbone.[2,3,5,7,27,28]

In the framework of the SCMF theory, the state of the system is described by the free energy functional

$$F[P[\gamma], c_s(\mathbf{r})] = kTN_p \int D\gamma\, (P[\gamma] \ln P[\gamma]) + kT \int_V d\mathbf{r}\, c_s(\mathbf{r}) \ln \phi_s(\mathbf{r}) + \int D\gamma\, P[\gamma]\, U[\gamma, c_s(\mathbf{r}), c(\mathbf{r})] \quad (2.1)$$

whose minimization gives the one chain probability distribution $P[\gamma]$ as well as the solvent number density $c_s(\mathbf{r})$. In this equation, γ denotes a given configuration of the chain, described by the set of the vectors pointing at the positions of all the N monomers of the chain $\{\mathbf{r}_i[\gamma]\}$. N_p is the number of chains in the volume and $\phi_s(\mathbf{r}) \equiv v_s c_s(\mathbf{r})$ is the solvent volume fraction, v_s being the volume of a solvent molecule. Furthermore, $D\gamma$ denotes an integration over all the self-avoiding configurations of the chain and kT has its usual meaning. In eq 2.1, $U[\gamma, c_s(\mathbf{r}), c(\mathbf{r})]$ is the energy of the system due to potential interactions. This term accounts for three types of contributions, that is, the interaction between monomers of the chain, interactions with monomers of other chains as well as the solvent molecules and, finally, the interactions with external fields. As in density functional theories, the hard-core repulsive interactions are not contained in eq 2.1 but are accounted for by means of the incompressibility constraint, expressed as

$$\phi(\mathbf{r}) + \phi_s(\mathbf{r}) = 1 \quad (2.2)$$

where ϕ, defined as

$$\phi(\mathbf{r}) \equiv N_p \int D\gamma\, P[\gamma] \sum_{i=1}^{N} v_p \delta(\mathbf{r} - \mathbf{r}_i[\gamma]) = v_p c(\mathbf{r}) \quad (2.3)$$

is the volume fraction of the polymers in the system. In this paper v_p is considered here as constant, for reasons of simplicity. According to ref 12, such an approximation does not properly describe the screening of the excluded volume correlations by the local monomer concentration in the semidilute regime. However, due to the marginal overlap of loops and tails at the inhomogeneous region, these correlations are not screened and this approximation suffices to quantitatively reproduce the volume fraction profiles.

Along this work, we have considered that the interactions between monomers and also between monomers and solvent are chosen to be identical. With a proper choice of the energy scale, the energetic term only contains the interaction between the monomers and the adsorbing wall, according to the expression

$$U[\gamma, c_s(\mathbf{r}), c(\mathbf{r})] = U_{ext}[\gamma] = \epsilon \int d\mathbf{r}\, \theta(d - |z - z_0|) \sum_{i=1}^{N} \delta(\mathbf{r} - \mathbf{r}_i[\gamma]) \quad (2.4)$$

where z_0 is the position of the hard wall, ϵ is the depth of the energy well, and d is the width of the well, $\theta(x)$ being the Heavyside function. The effect of the infinitely repulsive wall is implicitly taken into account by rejecting all conformations such that the center of at least one monomer i, say, is $|z_i| < |z_0|$.

Minimization of eq 2.1 subject to the constraint given in eq 2.2 gives the single-chain probability distribution

$$P[\gamma] = A e^{-H_{mf}[\gamma]/kT} \quad (2.5)$$

where A is the normalization constant and the mean-field Hamiltonian is given by

$$H_{mf}[\gamma] \equiv \int d\mathbf{r}\, [v_p \pi(\mathbf{r}) + \epsilon\theta(d - |z - z_0|)] \sum_{i=1}^{N} \delta(\mathbf{r} - \mathbf{r}_i[\gamma]) \quad (2.6)$$

In this last equation, notice the yet unknown constraint field $\pi(\mathbf{r})$ introduced as a Lagrange multiplier to satisfy the constraint given in eq 2.2. For the solvent number density profile one has, in turn

$$c_s(\mathbf{r}) = B e^{-v_s \pi(\mathbf{r})/kT} \quad (2.7)$$

where B is also a normalization constant fixed by the fact that the volume integration of eq 2.7 is precisely the total number of solvent molecules N_s.

Finally, to determine the spatial variation of the constraint field $\pi(\mathbf{r})$, we substitute in eq 2.2 the probability distribution function for the chain configuration, together with the solvent density profile, given in eqs 2.5 and 2.7, respectively. One finally writes

$$\frac{v_s}{l_s^3}e^{-v_s\pi(\mathbf{r})/kT}+\frac{V\phi^0}{N}\left[\frac{v_s/l_s^3}{1-\phi^0}\right]^{v_pN/v_s}\times \frac{\int D\gamma e^{-H_{mf}[\gamma]/kT}\sum_{i=1}^{N}\delta(\mathbf{r}-\mathbf{r}_i[\gamma])}{\int D\gamma}=1 \quad (2.8)$$

According to ref 12, in this last equation we have introduced the monomer volume fraction in a homogeneous system in equilibrium with our system, ϕ^0, as a free parameter. The point to point solution of eq 2.8 gives the profile of the constraint field $\pi(\mathbf{r})$ from which all the other properties can be determined.

To end this short overview of the SCMF technique, we calculate the configurational integrals by a Monte Carlo technique. Effectively, if one samples the configurational space of a self-avoiding chain producing a number Λ of different samples with a statistical weight $w[\gamma]$, then eq 2.8 can approximately be given by

$$e^{-v_s\pi(\mathbf{r})/kT}+\frac{V\phi^0}{N}\left[\frac{1}{1-\phi^0}\right]^{v_pN/v_s}\times \frac{\sum_{\alpha=1}^{\Lambda}e^{-H_{mf}[\gamma_\alpha]/kT}\sum_{i=1}^{N}\delta(\mathbf{r}-\mathbf{r}_i[\gamma_\alpha])/w[\gamma_\alpha]}{\sum_{\alpha=1}^{\Lambda}1/w[\gamma_\alpha]}=1 \quad (2.9)$$

where the factor v_s/l_s^3 has been absorbed into $\pi(\mathbf{r})$. Finally, any average of a given configurational space function $A(\mathbf{r}, \mathbf{r}_i[\gamma])$ is calculated from the relation

$$\langle A(\mathbf{r})\rangle=\frac{\int D\gamma e^{-H_{mf}[\gamma]/kT}A(\mathbf{r},\mathbf{r}_i[\gamma])}{\int D\gamma e^{-H_{mf}[\gamma]/kT}}\simeq \frac{\sum_{\alpha=1}^{\Lambda}e^{-H_{mf}[\gamma_\alpha]/kT}A(\mathbf{r},\mathbf{r}_i[\gamma_\alpha])/w[\gamma_\alpha]}{\sum_{\alpha=1}^{\Lambda}e^{-H_{mf}[\gamma_\alpha]/kT}/w[\gamma_\alpha]} \quad (2.10)$$

2.1. Numerical Calculation Details. The solution of the SCMF problem has been obtained here from a sampling of the configurational space of *off-lattice* polymers of 100 and 200 monomers, in a cubic box of size $L = 115.32l$ and $L = 226.92l$, respectively, l being the monomer length. The adsorbing wall has a thickness of $2.72l$ and is located at $z = 0$, occupying the center of the simulation box. The repulsive hard surfaces are then located at the planes $z \pm 1.36l$. The wall is rigid and cannot be penetrated by the chain beads such that $|z| < 1.86l = |z_0|$. We have introduced a square well potential at the surface of the plane, according to eq 2.4, whose width available to monomers is $d = 1.86l$ and different values of ϵ on the order of kT have been regarded. Since periodic boundary conditions are considered, the size of the box has been chosen large enough so that the chains never reach two surfaces at the same time.

The chains are described as pearl necklaces of nonoverlapping beads of diameter l, whose centers are separated a fixed distance equal to its diameter. The excluded volume per monomer has been taken as being independent of the conformation of the chain, and estimated to be $v_p = 1.86l^3$, assumed as constant throughout this work. This value corresponds to an estimate of the net excluded volume per monomer in a chain. As we have already noticed in ref 12 and mentioned above, this is the crudest approximation in this work.

The mean-field constraint $\pi(\mathbf{r})$ is considered as being a function of the coordinate z only, due to the symmetry of the system. The box has been divided then into layers of thickness $1.86l$, parallel to the plane, inside which π is taken as constant. This choice permits us to have a reasonable precision of the spatial variation of the fields and keeps eq 2.2 meaningful.

The Metropolis rule[29] is used to relax an originally chosen distribution of one-chain conformations to the desired biased distribution, according to the weight $w[\gamma]$, as has been described in detail ref 12. With the purpose of obtaining a statistically significant configurational file, we have chosen the Boltzmann weight

$$w[\gamma] \propto e^{-H_{mf}[\gamma]/kT} \quad (2.11)$$

where $H_{mf}[\gamma]$ is given in eq 2.6. The physical conditions chosen to relax the configurational file, where the one-chain biased conformations are stored, have been selected to be not too far from the physical conditions that we have analyzed, aiming at having significant enough samples for every case.

In the case that ideal instead of self-avoiding chains are generated in the sampling, the procedure followed is exactly the same. The main difference is found in the set of allowed conformations of the chain, something that will give significant differences when comparing the results obtained by means of both points of view.

3. Structure of the Adsorbed Layer

Let us introduce the characteristic length scales for polymer adsorption onto flat walls. First of all, the bulk correlation length ξ defines the distance at which density perturbations die out. The numerical value that we use in this section is calculated from the expression

$$\xi \equiv R_g\left(\frac{\phi^0}{\phi^*}\right)^{-3/4} \quad (3.12)$$

as obtained from scaling arguments for excluded volume chains,[4] with ϕ^0, the volume fraction of monomers in the bulk, and ϕ^*, the monomer volume fraction at the overlap distance c^*, defined as

$$c^* \equiv \frac{3N}{4\pi R_g^3} \quad (3.13)$$

where R_g is the radius of gyration of the chain numerically obtained in a homogeneous system. In the case of ideal chains, we still use eq 3.12 but with exponent $-1/2$ (instead of $-3/4$) and the radius of gyration correspond-

ing to that of an ideal chain. The overlap volume fraction is thus, $\phi^* = v_p c^*$.

Second, the thickness of the layer that we use in this work is obtained from the expression

$$\lambda^2 \equiv \frac{\int z^2 \phi_a(z)\, dz}{\int \phi_a(z)\, dz} \tag{3.14}$$

where ϕ_a is the volume fraction of monomers belonging to adsorbed chains. Similarly, from the volume fraction of monomers belonging to loops and tails their corresponding root-mean-square thickness, λ_t and λ_l respectively, are obtained.

As far as the inner structure of the adsorbed layer is concerned, it is customary to define *loops* as being portions of the adsorbed chain between two monomers in contact with the wall and *tails* as portions of the chain between the last adsorbed monomer and an end, while *trains* are sequences of monomers all in contact with the wall.[7] Here, however, we will make no distinction between trains and loops. The density profiles of monomers belonging to loops and to tails are, therefore, indicators of such an internal structure. Then, third and last, the crossover length z^* is defined in this work as the distance at which loop and tail monomer concentration profiles, c_l and c_t, respectively, cross each other,[8] separating the adsorbed layer into loop and tail sublayers. This can be formally stated as

$$c_l(z^*) = c_t(z^*) \tag{3.15}$$

With regard to the bulk concentration, different regimes are also usually distinguished. We have already defined the overlap concentration c^* in eq 3.13. Since the thickness of the layer scales as the size of the polymeric coil, R_g, the layer starts to be significantly affected by the presence of free chains in its vicinity when the bulk concentration approaches the overlap concentration, that is, when $\xi \sim R_g$. In the second place, the concentration c_1 is defined as the concentration at which $\xi \sim z^*$ so that the loop layer starts to merge into the bulk free polymers.[9] At higher polymer densities a concentration c_2 can also be introduced,[30] but its analysis lies beyond the scope of this work.

As far as the single-chain properties in a homogeneous system are concerned, in ref 12 our SCMF theory predicts a dependence of the end-to-end distance as well as the radius of gyration in the polymerization index N consistent with the self-avoiding chain statistics, i.e., $R_g \sim N^{3/5}$, if nonoverlapping chains are used in the sampling.[14,31] If overlapping chains are used instead, then the size of the polymeric coil scales as $N^{1/2}$, as corresponds to ideal chain statistics. Moreover, it has also been observed that the results are independent of the bulk monomer concentration, which implies that the model cannot properly account for the screening of the excluded volume correlations due to the simplistic formulation used in this work.[24] The reader is refered to ref 12 for a detailed discussion of this point. It is interesting to point out again the substantial difference between the use of self-avoiding vs overlapping chains in the sampling although the problem posed is identical at the mean field level. Effectively, if ideal chains are generated, all the effects of the excluded volume interactions are charged on the value of the molecular field π. Instead, when nonoverlapping conformations are considered, the molecular field π only accounts for the effect of the excluded volume interactions with monomers of other chains, since the intrachain interactions are exactly accounted for in the self-avoidance restriction.

Table 1. Volume Fraction at Contact with the Wall for Different Bulk Monomer Volume Fractions[a]

ϕ^0	ϕ^{SCMF}; $N = 100$	ϕ^{SCMF}; $N = 200$	ϕ^{MC}; $N = 200$
0.0026	0.47	0.48	0.62
0.022	0.50	0.50	0.62
0.11	0.56	0.56	0.67
0.81	0.91	0.91	0.92

[a] The results correspond to an adsorption energy $\epsilon = -1kT$, being obtained by means of single chain mean field (SCMF) for polymer lengths $N = 100$ and $N = 200$, as well as for Monte Carlo (MC) simulations for chains $N = 200$.

3.1. Comparison with Monte Carlo Simulations. Since one of the main objectives of this work is to check the ability of the SCMF method in producing reliable data on polymer adsorption, in what follows we will focus our analysis on the behavior of polymer adsorption as a function of the bulk concentration considering only a chain length $N = 200$. The comparison is done with data obtained from multichain lattice Monte Carlo simulations as given in refs 20 and 32. There are, however, intrinsic difficulties in the comparison due to the different nature of the models. We have chosen to identify the spacing of the cubic lattice defined in these references with our monomer length l. With this identification, the obtained radius of gyration from both methods for isolated chains are rather close, $R_g(MC)/l = 9.37$ as compared with $R_g(SCMF)/l = 11.29$ (one can also compare the parameters of the fitting $R_g/l = 0.42N^{0.594}$ given in ref 13, with those given in Table 1 of ref 12). Furthermore, we will compare the monomer volume fractions by simply multiplying our monomer concentration by the monomer volume $1.86l^3$, according to eq 2.3. For chains of 200 monomers, the overlap concentration is obtained from eq 3.13, giving $\phi^*(SCMF) = 0.061$ and $\phi^*(MC) = 0.051$.[13] In addition, the adsorption energy is chosen to be the same in both models and equal to $\epsilon = -1kT$. To compare the profiles we have chosen that the layer 1 in the MC simulations coincides with the external border of the adsorbing well. Obviously, this choice of monomer length and excluded volume parameter can distort the one to one comparison of the data. However, in our analysis we will center our attention on intrinsic properties of the layer, expressed in the natural lengths in each case in order to be independent of the particular values chosen. In addition, aiming at a closer comparison with MC data, we have introduced a finer division in the simulation box, with layers of thickness $0.93l$, inside which the value of the Lagrange multiplier field $\pi(z)$ has been calculated from the SCMF, eq 2.9.

In Figures 1−3, we show the comparison between monomer fraction profiles obtained from SCMF and MC simulations. In both methods the bulk monomer fraction is $\phi^0 = 0.0026$, corresponding to a very dilute solution. Despite the fact that the models used are rather different, the results for the total monomer volume fraction are very good, as can be seen in Figure 1. The difference in the volume fraction of monomers at contact with the wall could be attributed to the fact that the value of the volume fraction at this point is strongly dependent on microscopic details of the models, as far as the monomers and the potential well are concerned.

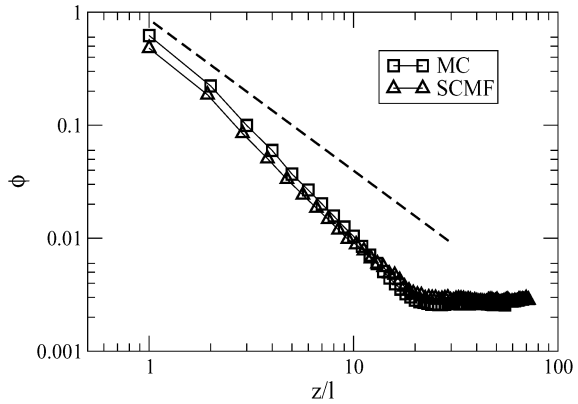

Figure 1. Comparison of the total monomer volume fraction profiles obtained from single chain mean field (SCMF) and Monte Carlo (MC) simulations. System conditions are $N = 200$, $\phi^0 = 0.0026$, and $\epsilon = -1kT$. The dashed line corresponds to a power law −4/3. Key: SCMF, triangles; MC, squares.

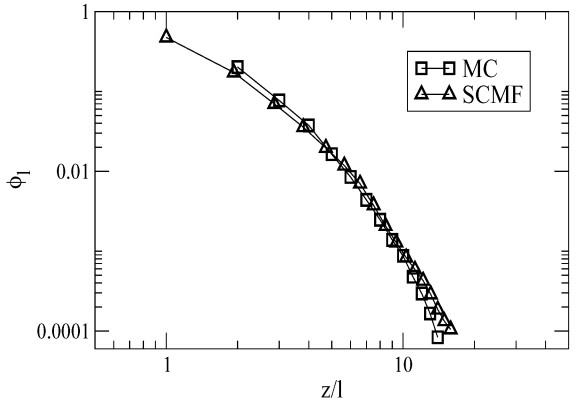

Figure 2. Comparison of the loop volume fraction profiles obtained from single chain mean field (SCMF) and Monte Carlo (MC) simulations. System conditions are $N = 200$, $\phi^0 = 0.0026$, and $\epsilon = -1kT$. Key: SCMF, triangles; MC, squares.

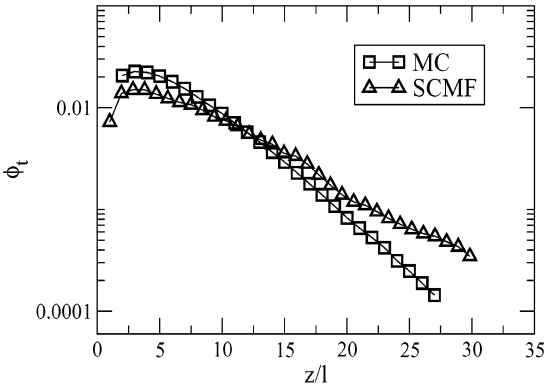

Figure 3. Comparison of the tail volume fraction profiles obtained from single chain mean field (SCMF) and Monte Carlo (MC) simulations. System conditions are $N = 200$, $\phi^0 = 0.0026$, and $\epsilon = -1kT$. Key: SCMF, triangles; MC, squares.

Table 1 summarizes the volume fractions at contact with the wall for four different concentrations.

Despite the numerical differences in the volume fraction at contact with the wall, MC and SCMF results are consistent. In the case of SCMF values for $N = 100$ and $N = 200$, they indicate that this magnitude is rather independent of the size of the chain and only depends on the bulk concentration, for fixed adsorption energy ϵ. Furthermore, it is interesting to observe that, with a smooth increase of the bulk concentration, both models show a saturated surface at high bulk monomer concentration. However, a detailed analysis of this effect lies beyond the scope of this work.

The straight dashed line plotted in Figure 1 corresponds to a slope of −4/3 which is the scaling prediction for $N \to \infty$, according to $c(z) \sim z^{(1-\nu d)/\nu}$, ν being the Flory exponent and d the dimensionality of the space. The agreement between MC and our SCMF results is very good. The analysis of both sets of data indicate that the existence of a power-law regime is not obvious (the exponent in the central region of the profiles is near −2, and is less negative near contact). Without any doubt, the decay presented in both results is steeper than the scaling predictions, $N \to \infty$, for self-avoiding chains. Although this decay seems to be close to that predicted by scaling arguments for ideal chains (z^{-2}, with $d = 4$ and $\nu = 1/2$ in the scaling formula), one should not infer that the decay is correctly given by Markovian mean-field calculations. Effectively, the solution of the SCMF equations with Markovian overlapping chains shows an even steeper decay for this chain length. The same kind of behavior is observed in the solution obtained with the Scheutjens−Fleer method.[20] This power-law regime, therefore, depends on bulk concentration for such moderately long chains, very far from the asymptotic limit where the scaling results would be valid. This effect has already been discussed in refs.[13,32] and our data are in agreement with this fact.

In Figure 2, we compare the SCMF and MC results for the loop monomer volume fraction profile using a logarithmic scale. The MC data suppresses the value at contact with the wall, attributed to trains. We observe that again, the agreement is very good, although the SCMF produces a slightly thicker layer. It is also noticeable that no power-law regime is identifiable in any of the data sets. Although scaling predicts a power-law decay of $-4/3$ for this quantity near the wall, the observed behavior in the numerical data is in agreement with a faster initial decay, close to a power of −3.

Figure 3 represents the volume fraction profiles of monomers belonging to tails in a semilogarithmic scale. In this profile, the differences between the SCMF and MC results are more pronounced. The decay in the *distal* part of the layer is close to a single-exponential decay in the MC data. SCMF data is affected by statistical inaccuracy at the low-density part of the profile, but it is rather obvious that the data shows a much slower decay. The exponential fit $\phi_t = A \exp(-\alpha z)$ to the distal region of the tail layer gives an exponent $\alpha = -0.244$ for the MC data, and −0.160 for the SCMF. This difference can be analyzed from another perspective, taking into account the fact that this exponent has to be inversely proportional to the characteristic size of the tails which can be defined as $lN_t^{3/5}$. Thus, we can write

$$\frac{\alpha(\mathrm{MC})}{\alpha(\mathrm{SCMF})} = \frac{0.244}{0.160} = 1.53 \simeq \left(\frac{N_t(\mathrm{SCMF})}{N_t(\mathrm{MC})}\right)^{3/5} \qquad (3.16)$$

where the Flory exponent $3/5$ has been used since the bulk is very dilute and there is no physical screening of the excluded volume correlations. From this equation we can infer that $N_t(\mathrm{SCMF})/N_t(\mathrm{MC}) \simeq 2.03$, which means that the size of the tails predicted is approximately twice that of the MC data. For consistency, we have verified, in addition, that our tail profile for $N = 100$ agrees very well with the tail profile obtained from

Table 2. Characteristic Dimensions of the Adsorbed Layer, in Units of *l*, Obtained from Single Chain Mean Field (SCMF) and Monte Carlo (MC) Methods, for Various Bulk Volume Fractions

ϕ^0		z^*	λ	λ_l	λ_t	ξ	R_g
0.0026	MC	4.79	3.85	3.19	8.35	91.50	9.76
	SCMF	7.53	4.45	4.26	11.50	121.53	11.29
0.022	MC	4.71	5.36	3.58	9.91	18.44	9.76
	SCMF	7.60	6.91	4.41	14.88	24.49	11.29
0.11	MC	4.04	7.33	4.09	10.77	5.56	9.76
	SCMF	6.32	10.66	5.21	15.91	7.33	11.29
0.81	MC	3.44	7.93	4.62	9.56	1.25	9.76
	SCMF	5.38	13.52	6.23	16.19	1.65	11.29

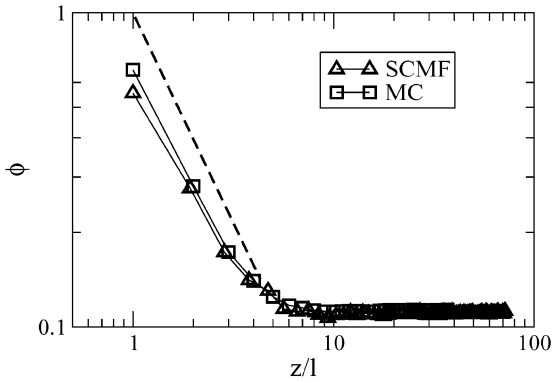

Figure 4. Monomer volume fraction profiles obtained from single chain mean field (SCMF) and Monte Carlo (MC) simulations. System conditions are $N = 200$, $\phi^0 = 0.11$, and $\epsilon = -1kT$. The dashed line corresponds to a power law $-4/3$. Key: SCMF, triangles; MC, squares.

MC data but with $N = 200$, confirming our estimation of the size of the tails. This discrepancy of a factor near 2 is surprising. Although the statistics in the distal part of the tail profile is rather poor, where the volume fraction is around 10^{-3} and below, the overall discrepancy suggests that the decay of the tail profile for this system has to be more carefully studied. In fact, as we will see later on, the agreement of the tail profile between our SCMF calculations with overlapping chains and the SCF results agree very well except for the distal region, which suggests the correctness of our predictions in the region near the wall for the tail profile also in the case of self-avoiding chains under discussion. Other sources of disagreement are the differences between the radii of gyration between MC and in our SCMF, although this is too small to justify the difference.

In Table 2, the characteristic lengths of the layer for four different concentrations are shown. The thickness of the layer for $\phi^0 = 0.0026$ is found to be $\lambda = 4.45l$ while for the tails its value rises up to $\lambda_t = 11.50l$, which is close to the value of the radius of gyration of the chain, $11.29l$. Notice also that the crossover length $z^* = 7.53l$ is larger than the thickness of the layer, which corresponds to what is expected in the starved regime.[9] Thus, the profile in the central and distal regions is dominated by one single length, namely λ[33] or, equivalently, z^*. In the limit $N \to \infty$, the crossover length in the central regime is z^* while λ is important only near the cutoff of the layer in the distal region, since $z^* \ll \lambda$.[8,9] For our range of chain sizes, both characteristic lengths are comparable.

Figures 4−6 correspond to a higher volume fraction $\phi^0 = 0.11$, above the overlap concentration, considering the same chain length and adsorption energy as before. The general analysis goes along the same lines as in the previous case. The total monomer volume fraction

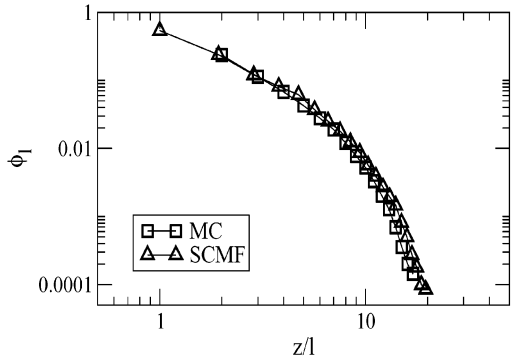

Figure 5. Loop volume fraction profiles obtained from single chain mean field (SCMF) and Monte Carlo (MC) simulations. System conditions are $N = 200$, $\phi^0 = 0.11$, and $\epsilon = -1kT$. Key: SCMF, triangles; MC, squares.

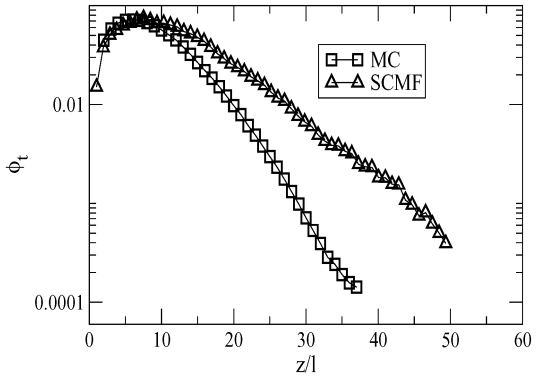

Figure 6. Tail volume fraction profiles obtained from single chain mean field (SCMF) and Monte Carlo (MC) simulations. System conditions are $N = 200$, $\phi^0 = 0.11$, and $\epsilon = -1kT$. Key: SCMF, triangles; MC, squares.

of the adsorbed chains obtained from SCMF deviates slightly from the MC results in all the regimes. This fact is reminiscent of the nonscreening of the excluded volume correlations in semidilute solutions in our methodology. Effectively, the increase of the osmotic pressure with concentration in the bulk favors more compact configurations, due to the effective reduction of the excluded volume per chain. Our model, with a constant excluded volume per monomer, cannot properly account for this effect. The difference, however, is not significant for the conditions analyzed here.

For this bulk concentration ($\phi^0 = 0.11$), the major part of the tail layer is embedded in the bulk fluid. Effectively, the bulk correlation length has been calculated from eq 12 obtaining $\xi = 7.33l$, while the thickness of the layer is $\lambda = 10.66l$ (see Table 2). The thickness of the tail profile is in turn $\lambda_t = 15.91l$. In this case, the comparison between MC and SCMF data for the tail monomer profile is better near contact. However, the decay of the tails is significantly slower for the SCMF data. This is also influenced by the nonscreening of the excluded volume correlations of the model, although a lack of representative statistics in the distal region seems to be the major cause. Finally, the calculated value of the crossover length is $z^* = 6.32l$. Notice that ξ is very close to z^* which indicates that this concentration is very close to $\phi_1 = \nu_p c_1$ at which the loop layer enters into contact with the bulk polymers.

In general, one can say that the SCMF and MC results increasingly deviate as the concentration increases and that the behavior of the MC chains tends to be more ideal as the concentration approaches that

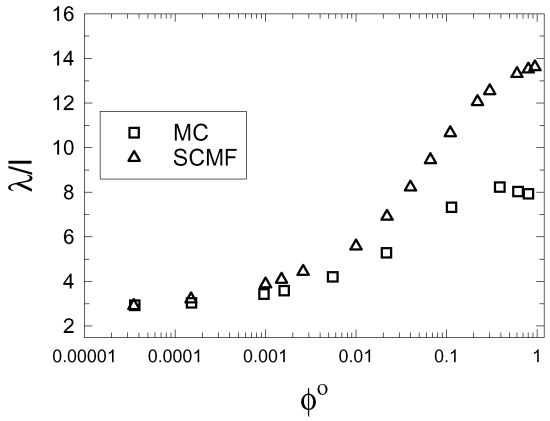

Figure 7. Variation of the rms thickness as a function of bulk volume fraction. Conditions of the system: $N = 200$ and $\epsilon = -1kT$. Single chain mean field results (SCMF) are represented by triangles and Monte Carlo results (MC) by squares.

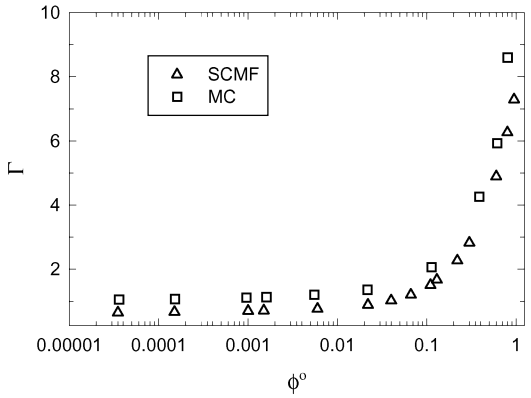

Figure 8. Variation of the adsorbance (number of monomers per l^2) in function of bulk volume fraction. Conditions of the system: $N = 200$ and $\epsilon = -1kT$. Single chain mean field results (SCMF) are represented by triangles and Monte Carlo results (MC) by squares.

of the melt. To illustrate this point, in Figure 7, we present the dependence of the root-mean-square (rms) thickness of the adsorbed layer with the bulk volume fraction, as obtained from both SCMF and MC methods. The overall thickness of the layer increases with concentration essentially due to the progressive competition between chains to cover the same surface, which induces a decrease in the adsorption energy per chain. The rise becomes important near and above the overlap concentration ($\phi^* = 0.061$ from SCMF data used here). The discrepancy between the two curves is due to the different extension of the tail layer between MC and SCMF data. The loop layer is only slightly influenced by the bulk monomer density up to concentrations close to that of the melt. Tails contribute significantly to the overall thickness of the layer due to their long extension, despite the fact that their contribution to the density profile is very low. In the SCMF calculations, there is no shrinkage of the conformations due to the nonscreening of the excluded volume correlations, leading to larger values of the calculated thickness. Notice that this shrinkage of the overall layer is responsible, for instance, for the slight decrease in the layer thickness of the MC data at high concentrations.

In Figure 8, we present the adsorbance, defined from the adsorbed chain monomer concentration $c_a(z)$, as

$$\Gamma = \int_0^\infty c_a(z)\, dz \tag{3.17}$$

as a function of the concentration, for the conditions of chain length and adsorption energy previously used. We observe a good agreement between the qualitative behavior displayed by both series of data. The increase of the adsorbance starts near the crossover concentration, where the competition between the polymers to cover the surface causes them to prefer more elongated conformations, with larger loops and tails. This is the same effect that causes the thickness of the layer to increase, as has been previously mentioned.

3.2. Comparison with Markovian Self-Consistent Field Calculations. To end this section, we have performed SCMF calculations with overlapping chains, to compare with results obtained by means of the SCF method of Scheutjens and Fleer.[7] In this limit, both mean field theories should be equivalent since the chain propagator is Markovian. In all cases we have used the same set of parameters as before, $N = 200$, $\epsilon = -1kT$ and different bulk monomer volume fractions. For the SCF model, the data correspond to the same value l for the monomer length, identifying the parameter χ_s with the adsorption energy ϵ of our calculations.[33,34]

Parts a and b of Figure 9 show, respectively, loop and tail monomer volume fraction profiles from SCMF equations, using overlapping chains in the sampling, in comparison with the SCF data of Scheutjens and Fleer, at very dilute solution $\phi^0 = 0.0026$. To emphasize the role played by the excluded volume correlations, i.e., the Markovian or non-Markovian nature of the chains, in the same figures we have plotted (lines without symbols) the MC profiles as well as the SCMF results with self-avoiding chains. Focusing our attention on the Markovian data, one can see in Figure 9a that the agreement between SCF and SCMF data is excellent. Moreover, we observe a significant difference between self-avoiding and overlapping chain calculations, the latter always presenting a much faster decay, as has already been indicated in the discussion of Figure 1.

In the case of the tail monomer volume fraction profiles given in Figure 9b, the agreement between SCF and SCMF calculations is very good in one decade, and deviates at the distal part of the layer, where the values of the volume fraction due to tails are very low. At has been already pointed out, we attribute this discrepancy to the lack of statistical sampling of the data. Again, the corresponding values obtained from nonoverlapping chains are significantly higher, indicating a less compact structure caused by the direct excluded volume correlations along the chain backbone. In this figure, the already mentioned overall discrepancy of the MC data of ref 13 for this particular set is rather noticeable, which seems to better correspond to chains of $N = 100$ monomers than $N = 200$.

Higher bulk concentrations lead to results that are qualitatively similar to those shown and will not be further discussed. Bitsanis and collaborators[20,32] have already pointed out this general difference in the behavior of the adsorbed layer by directly comparing SCF calculations and MC simulations. One of the more important results of this work is in fact to show that the effect is entirely caused by the intrachain excluded volume correlations, neglected in the classical SCF approach. Effectively, the SCMF formalism disregards the interchain correlations as in SCF calculations. However, the fact that the reference chain can be

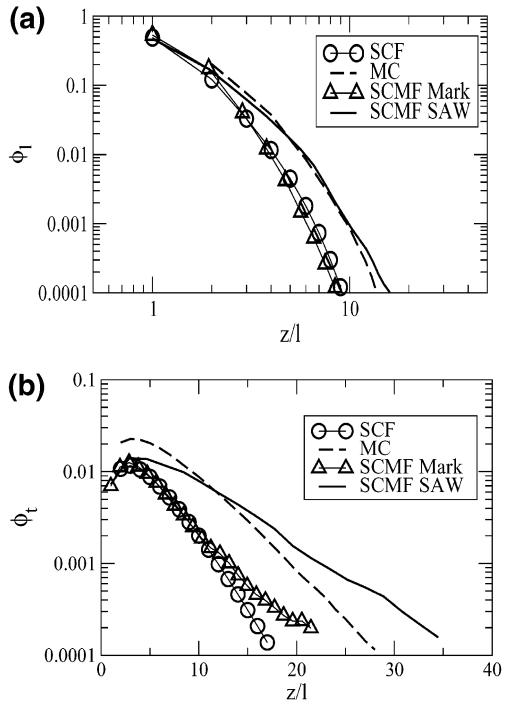

Figure 9. Loop (a) and tail (b) monomer volume fraction profiles corresponding to markovian and self-avoiding walk (SAW) chains. System conditions are $N = 200$, $\phi^0 = 0.0026$, $\epsilon = -1kT$. Markovian results are obtained from the Scheutjens−Fleer method (SCF) (circles) and single chain mean field (SCMF) method (triangles). In the case of the self-avoiding walk results (SAW), they are obtained from Monte Carlo method (MC), dashed line, simulations and single chain mean field method (SCMF), full line.

nonoverlapping permits us to properly account for the correlations along the chain backbone, unlike the classical mean field theories based on the solution of the Edwards equation.

4. Conclusions

The main purpose of this paper has been to present the results obtained from the SCMF method for the case of the adsorption of polymers at flat surfaces, in comparison with two well-known methodologies, which respond to two different approaches to the problem. We have been able to show the efficiency of the *importance sampling* method, introduced in ref 12, applied in the framework of the known single chain mean field theory for the reversible polymer adsorption problem. Furthermore, from our methodology, it has been possible to obtain results corresponding to both self-avoiding and overlapping Markovian chains, that have been compared, respectively, with other known methodologies such as Monte Carlo simulations and the self-consistent field method of Scheutjens and Fleer. We will briefly discuss both points in what follows.

The advantage of the importance sampling is that all the samples of the one-chain configurational space contribute to the averages with the same weight, inducing a reduction of the number of samples required for a problem such as polymer adsorption, characterized by a narrow well near a repulsive wall. Our results have been obtained with a reduced number of configurations (2×10^4), that can be handled by common PC's. To relax the probability distribution toward the desired bias, we have introduced a Metropolis rule, viewing the configurational file as a pseudo-system of independent chains in a biasing field. This procedure is clearly time consuming although efficient enough. In addition, the procedure permits us to arrive at the optimal sampling for each situation, something that has allowed us to make a drastic reduction of the computer memory used in our calculations. Other methodologies, such as the Rosenbluth chain regrowth algorithm,[35] are actually being used in this context, with much less intensive use of CPU time.[36]

As far as the results are concerned, we have shown that the agreement between the SCMF results with self-avoiding chains and MC simulations is very good, despite the disparate nature of the models used in each case. We have obtained practically the same density dependence as found in MC simulations in both dilute as well as semidilute solutions, for several properties such as monomer density profile, loop density profile, adsorbance, etc. However, the simplistic model used here is unable to reproduce the screening of the excluded volume correlations along the chain. The SCMF methodology, with an appropriate model with conformation-dependent excluded volume, should be able to also describe this phenomenon. The nonscreening of excluded volume correlations leads to swollen chains under all situations, independently of the local monomer volume fraction. This effect is especially noticeable in homogeneous concentrated solutions, where the chain statistics is physically expected to be Gaussian (ideal), but our SCMF results give self-avoiding statistics, typical of dilute solutions. Hence, the density profiles are slightly thicker than found in MC simulations, especially for semidilute solutions. This fact has already been recognized in the literature.[24,26] A refined model to overcome this drawback will be addressed elsewhere. The marginal overlap of loops and tails in the adsorbed layer is responsible for the excellent agreement between our SCMF and MC simulations in the inhomogeneous region.[4] Notice that the screening of the excluded volume correlations is a genuine issue of self-avoiding chain statistics which has no counterpart in ideal chain problems and can by no means be addressed in the context of the SCF calculations.

Last, but not least, we have compared the results of our mean-field approach when overlapping chains are used. This procedure renders our approach conceptually equivalent to the Markovian SCF methodology, based on the Edwards propagator, widely used in polymer chemical physics. Effectively, the profiles predicted by matching the parameters of the model, with no further adjustable parameters, is excellent. Only the distal part of the adsorbed layer is affected in our case by a lack of representative statistics, inducing deviations in the tail profile in the last part. The formal relationship between the SCMF and the SCF methods based on ideal chain statistics is rather straightforward and has been already addressed in refs 24 and 26. Here we have shown that the fundamental difference between the two methods is the explicit consideration of the correlations along the chain in the former. The SCF methods based on the Edwards propagator make explicit use of the Markovian character of the chain propagator[28] through a differential (or difference, in the Scheutjens−Fleer method) equation for the chain propagator. The monomers interact only with the self-consistent field. On the other hand, the SCMF technique with self-avoiding configurations takes into account the non-Markovian nature of the chain propagator with excluded volume interactions.

Of course, when this point is relaxed by allowing the generation of chains without internal excluded volume interactions, the Markovian character of these conformations is recovered, and therefore, Markovian SCMF and SCF results completely agree.

By our analysis, it is thus made clear the nature of the SCMF calculations and the importance of the one-chain excluded volume correlations in the problem of polymer adsorption. The agreement between our SCMF calculations with self-avoiding chains and the MC simulations indicate that the structure of the layer is mainly determined by the excluded volume correlations along one single chain, the many chain correlations being of lesser importance. This behavior has its roots in the local swelling of the chain, correctly accounted for by the SCMF equations and the marginal overlap of loops and tails at the inhomogeneous layer.

It is thus expected that a further development of the method, to overcome the weaknesses of the model as well as the efficiency in the sampling of the one-chain configurational space, will lead to the possibility of performing quantitative predictions of large systems.

Acknowledgment. The authors wish to thank Drs. Albert Johner and E. Blokhuis for many fruitful discussions but, above all, for their friendship. Dr. Jan van Male is acknowledged for providing us with the SCF data and also for clarifying discussions. We are also indebted to Dr. Jason de Joannis for his MC data used for comparison. This work has been supported by the Ministerio de Ciencia y Tecnologıa of the Spanish Government through grants PPQ2000-2888E and PPQ2001-0671. S.D.-O. also acknowledges the Universitat Rovira i Virgili for financial support. J.B.A. also wishes to thank the support of the Dutch NWO during his stay at Leiden University.

References and Notes

(1) Jones, I.; Richmond, P. *J. Chem. Soc., Faraday Trans. 2* **1977**, *73*, 1062.
(2) Edwards, S. F. *Proc. Phys. Soc. (London)* **1965**, *85*, 613.
(3) Edwards, S. F. *Proc. Phys. Soc. (London)* **1966**, *88*, 265.
(4) de Gennes, P. G. *Scaling Concepts in Polymer Physics*; Cornell University Press: Ithaca, NY, 1979.
(5) Lifshitz, I. M.; Grosberg, A. Yu.; Khokhlov, A. R. *Rev. Mod. Phys.* **1989**, *50*, 683.
(6) de Gennes, P. G. *Macromolecules* **1981**, *14*, 1637.
(7) Fleer, G. J.; Cohen-Stuart, M. A.; Scheutjens, J. M. H. M.; Cosgrove, T.; Vincent, B. *Polymers at Interfaces*; Chapman and Hall: London, 1993, and references therein.
(8) Semenov, A. N.; Joanny, J. F. *Europhys. Lett.* **1995**, *29*, 279.
(9) Semenov, A. N.; Bonet Avalos, J.; Johner, A.; Joanny, J. F. *Macromolecules* **1996**, *29*, 2179.
(10) Johner, A.; Bonet Avalos, J.; van der Linden, C. C.; Semenov, A. N.; Joanny, J. F. *Macromolecules* **1996**, *29*, 3629.
(11) Auvray, L.; Cotton, J. P. *Macromolecules* **1987**, *20*, 202.
(12) Bonet Avalos, J.; Díez-Orrite, S.; Mackie, A. D. *Macromolecules* **2004**, *37*, 0000.
(13) de Joannis, J.; Ballamundi, R. K.; Park, C.-W.; Thomatos, J.; Bitsanis, I. A. *Europhys. Lett.* **2001**, *56*, 200.
(14) des Cloizeaux, J.; Jannink, G. *Les polymres en solution: leur modlisation et leur structure*; Les editions de Physique: Les Ulis, France, 1988.
(15) Eisenriegler, E. *Polymers near Interfaces*; World Scientific Publishing: Singapore, 1993.
(16) Zajac, R.; Chakrabarti, A. *J. Chem. Phys.* **1996**, *104*, 2418.
(17) Jiang, J.; Liu, H.; Hu, Y. *Macromol. Theory Simul.* **1998**, *7*, 105.
(18) Lai, P.-Y. *J. Chem. Phys.* **1995**, *103*, 5742.
(19) Milchev, A.; Binder, K. *Macromolecules* **1996**, *29*, 343.
(20) de Joannis, J.; Park, C.-W.; Thomatos, J.; Bitsanis, I. A. *Langmuir* **2001**, *17*, 69.
(21) Ben-Shaul, A.; Szleifer, I.; Gelbart, W. M. *J. Chem. Phys.* **1985**, *83*, 3597.
(22) Carignano, M. A.; Szleifer, I. *J. Chem. Phys.* **1992**, *98*, 5006.
(23) Szleifer, I. *Biophys. J.* **1997**, *72*, 595.
(24) Szleifer, I.; Carignano, M. A. In *Advances in Chemical Physics*; Prigogine, I., Rice, S. A., Eds.; John Wiley and Sons: New York, 1996.
(25) Mackie, A. D.; Panagiotopoulos, A. Z.; Szleifer, I. *Langmuir* **1997**, *13*, 5022.
(26) Carignano, M. A.; Szleifer, I. *J. Chem. Phys.* **1993**, *98*, 5006.
(27) Lifshitz, I. M. *Soviet Physics JETP* **1969**, *28*, 1280.
(28) Doi, M. *Introduction to polymer physics*, Clarendon Press: Oxford, England, 1996.
(29) Frenkel, D.; Smit, B. *Understanding Molecular Simulation*; Academic Press: San Diego, CA, 1996.
(30) Marques, C. M.; Joanny, J. F. *J. Phys. (Fr.) I* **1988**, *49*, 1103.
(31) Flory, P. F. *Principles of Polymer Chemistry*; Cornell University Press: Ithaca, NY, 1953.
(32) de Joannis, J. Equilibrium properties of polymer solutions at surfaces: Monte Carlo simulations. Ph.D. Thesis, University of Florida, 2000.
(33) Fleer, G. J.; van Male, J.; Johner, A. *Macromolecules* **1999**, *32*, 825.
(34) Fleer, G. J.; van Male, J.; Johner, A. *Macromolecules* **1999**, *32*, 845.
(35) Rosenbluth, M. N.; Rosenbluth, A. W. *J. Chem. Phys.* **1955**, *23*, 356.
(36) Al-Anber, Z.; Bonet Avalos, J.; Mackie, A. D. *J. Chem. Phys.* **2003**, in preparation.

MA034349T